

High Pressure Isosymmetric Phase Transition of Biurea

SUPPLEMENTARY INFORMATION

Craig L Bull,^a Nicholas P Funnell,^a Christoper J Ridley,^a
Colin R. Pulham,^b Paul DeCoster,^b James Tellam,^a and William G Marshall^a

^a ISIS Facility, Rutherford Appleton Laboratory, Harwell Science and Innovation Campus,
Didcot, OX11 0QX, UK

^b EastCHEM School of Chemistry, Joseph Black Building, David Brewster Road, Edinburgh, EH9 3FJ, UK

*To whom correspondence should be addressed;

E-mail: craig.bull@stfc.ac.uk

Submitted to CrystEngComm.

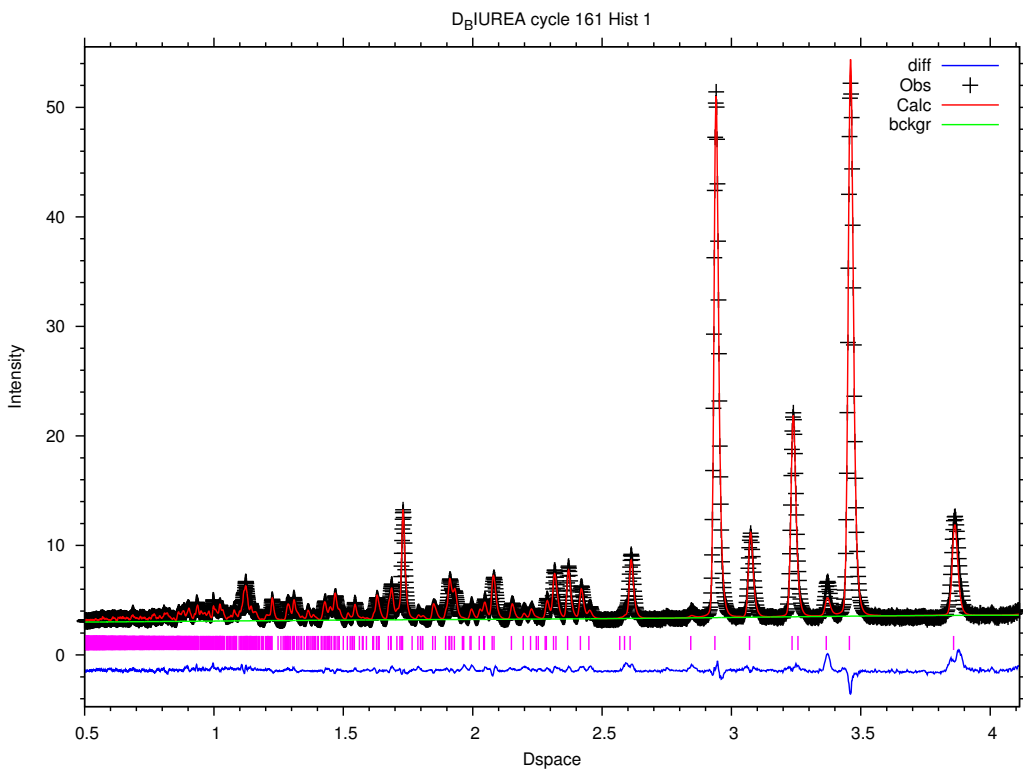


Figure S1: Neutron–powder diffraction measurement and associated Rietveld refinement of perdeuterated biurea within a vanadium can at ambient pressure and temperature. The black crosses indicate the data, the red line the fit to the data, vertical pink tick marks show the expected positions of the reflections and the blue trace shows the difference between the data and fit. Data have been collected on the PEARL instrument.

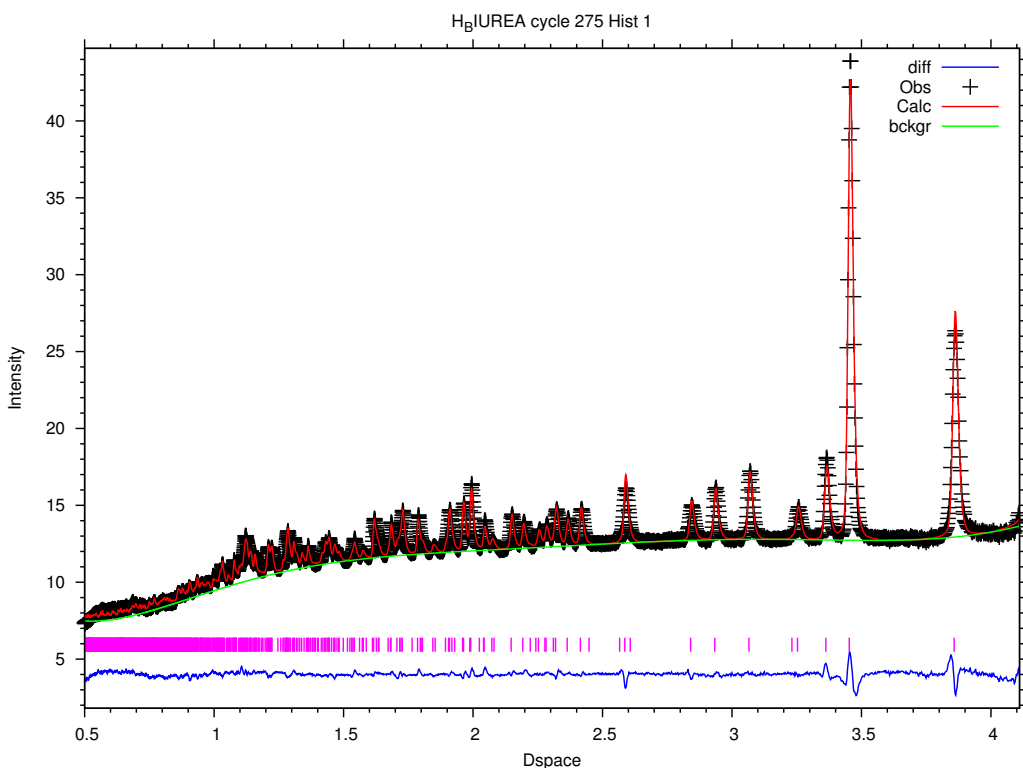


Figure S2: Neutron–powder diffraction measurement and associated Rietveld refinement of perhydrogenated biurea within a vanadium can at ambient pressure and temperature. The black crosses indicate the data, the red line the fit to the data, vertical pink tick marks show the expected positions of the reflections and the blue trace shows the difference between the data and fit. Data collected on the PEARL instrument. Note the high background characteristic high incoherent scattering of hydrogen.

Table S1: Structural parameters of perhydrogenated (as received) and perdeuterated biurea determined by Rietveld refinement at ambient conditions in a vanadium can. Measurements performed on the PEARL instrument (details in main manuscript).

Parameter	Biurea-h ₆			Biurea-d ₆		
	<i>a</i> (Å)	<i>b</i> (Å)	<i>b</i> (Å)	<i>a</i> (Å)	<i>b</i> (Å)	β (°)
Lattice parameter	9.3327(4)	4.6377(2)	11.4737(6)	81.977(4)	9.3387(4)	4.6440(2)
Unit Cell Volume (Å ³)	491.72(3)			493.11(2)		
				<i>x</i>	<i>y</i>	<i>z</i>
C	0.4010(4)	0.1883(8)	-0.0981(4)	0.4022(4)	0.1995(9)	-0.0965(3)
H(D)	0.3752(10)	0.478(2)	0.0312(8)	0.3741(4)	0.5037(9)	0.0327(3)
H(D)	0.2287(1)	-0.0222(3)	-0.1442(8)	0.2242(6)	-0.0106(14)	-0.1446(4)
H(D)	0.3977(9)	-0.0907(2)	-0.2286(8)	0.3889(7)	-0.0945(1)	-0.2332(4)
N	0.3252(4)	0.3399(8)	-0.0074(3)	0.3247(3)	0.3341(6)	-0.0068(3)
N	0.3323(4)	0.0094(9)	-0.1615(4)	0.3349(4)	0.0207(9)	-0.1598(3)
O	0.5408(6)	0.2373(12)	-0.1199(4)	0.5363(5)	0.2347(12)	-0.1188(4)

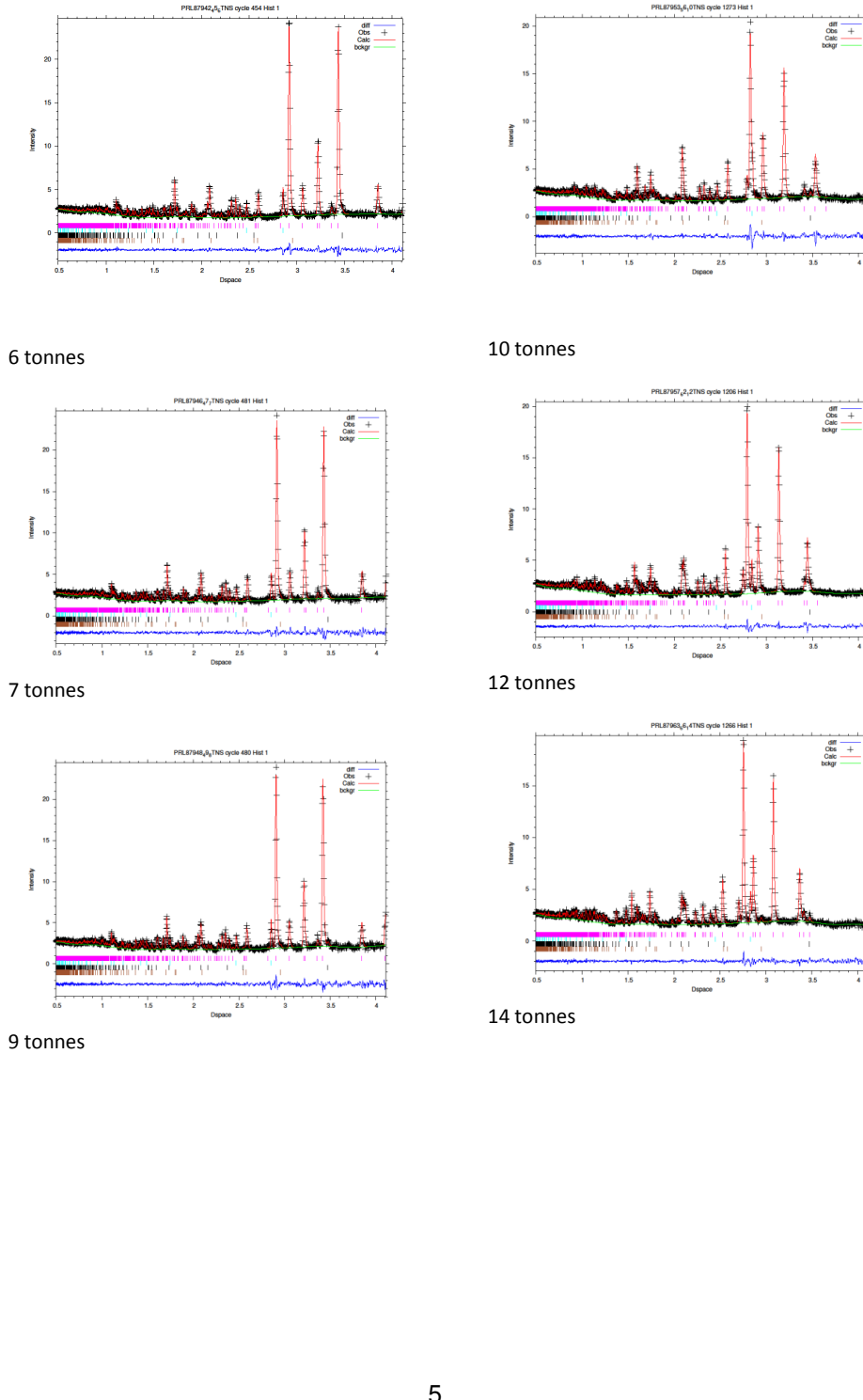


Figure S3: Rietveld refinements of perdeuterated biurea at pressure in phase I and II. The change in diffraction patterns is clearly seen between between phase I and II between 9 and 10 tonnes applied load (0.5 and 0.62 GPa respectively).

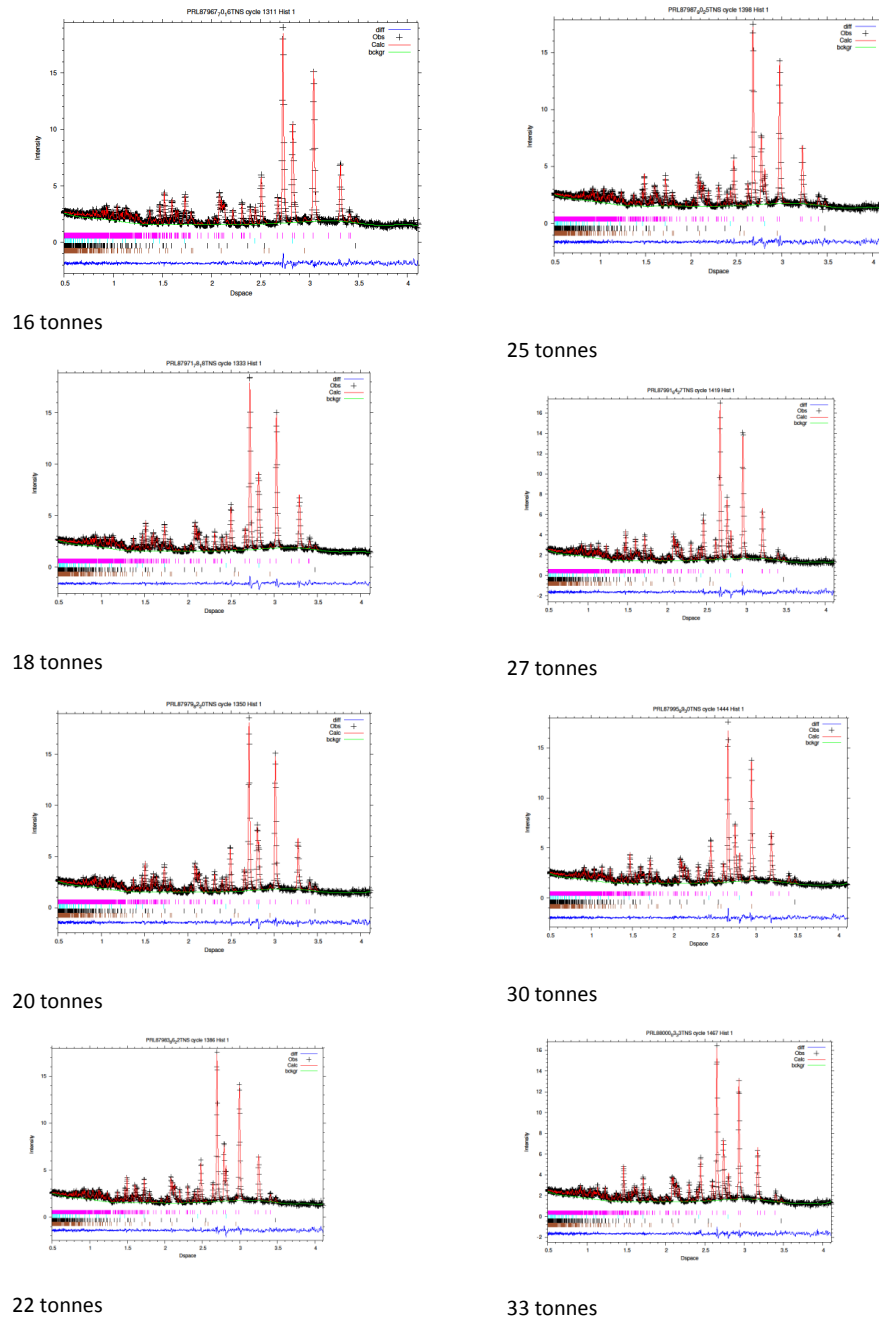


Figure S4: Rietveld refinements of phase II of perdeuterated biurea at pressure.

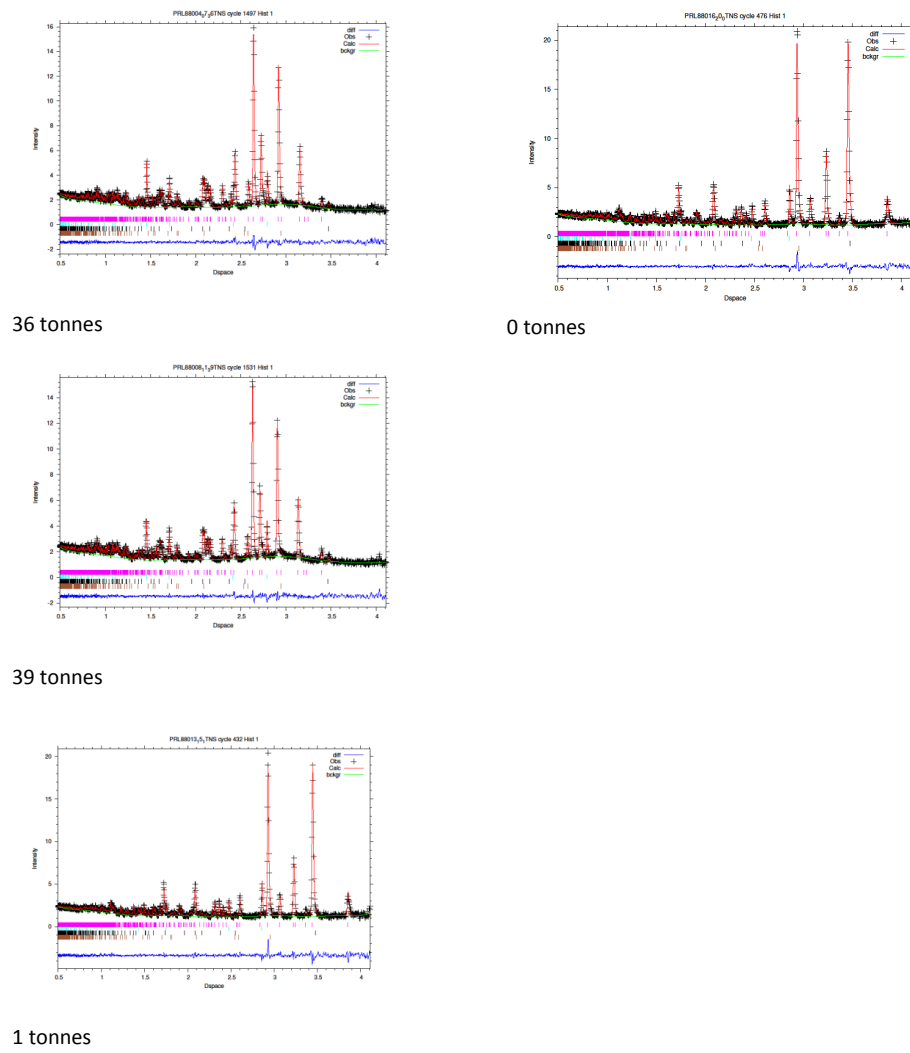


Figure S5: Rietveld refinements of phase II of perdeuterated biurea at pressure and subsequent recovery to phase I at 1 and 0 tonnes.

Table S2: Refinement details for high-pressure data collections of perdeuterated biurea ($\text{C}_2\text{D}_6\text{N}_4\text{O}_2$) in the monoclinic space group $I2/a$.
 Formula Weight 124.13 (g mol $^{-1}$). See main manuscript for further experimental details and CIFs CCDC 1935728–1935746.

Load (tonnes)	Pressure (GPa)	Phase	a-axis (Å)	b-axis (Å)	c-axis (Å)	β (°)	Volume (Å 3)	R_{wp}	G–o–f
6	0.02	I	9.3370(5)	4.6053(2)	11.4184(6)	82.134(5)	486.37(3)	2.94	1.120
7	0.026	I	9.3380(6)	4.5938(3)	11.4034(7)	82.154(6)	484.59(3)	3.70	0.934
8	0.36	I	9.3394(7)	4.5765(3)	11.3816(7)	82.160(6)	481.92(3)	4.22	0.96
9	0.5	I	9.3429(5)	4.5550(2)	11.3567(6)	82.183(5)	478.82(3)	3.29	1.146
10	0.62	II	9.4872(7)	3.81402(19)	12.8589(10)	77.936(7)	455.01(4)	3.80	1.495
12	0.90	II	9.4850(5)	3.70468(11)	12.9889(7)	77.632(4)	445.83(2)	2.66	1.593
14	1.31	II	9.4768(5)	3.61125(13)	13.0677(8)	77.463(5)	436.55(3)	3.22	1.057
16	1.63	II	9.4644(5)	3.55030(11)	13.1017(7)	77.388(4)	429.62(2)	3.20	1.000
18	1.87	II	9.4568(4)	3.51779(9)	13.1178(6)	77.346(4)	425.79(2)	2.56	1.824
20	2.02	II	9.4526(5)	3.49778(11)	13.1229(8)	77.341(5)	423.34(3)	3.33	1.136
22.5	2.25	II	9.4444(5)	3.46902(11)	13.1315(7)	77.318(4)	419.73(2)	3.29	1.113
25	2.53	II	9.4344(5)	3.44007(10)	13.1345(7)	77.317(4)	415.88(2)	3.42	1.069
27.5	2.81	II	9.4251(5)	3.41438(10)	13.1382(7)	77.309(4)	412.47(2)	3.34	1.009
30	3.04	II	9.4190(5)	3.39405(10)	13.1379(7)	77.310(4)	409.74(2)	3.36	1.126
33	3.28	II	9.4113(5)	3.37412(10)	13.1358(7)	77.317(4)	406.95(2)	3.46	1.008
36	3.57	II	9.4033(5)	3.35415(10)	13.1320(7)	77.321(5)	404.09(2)	3.55	1.062
39	3.89	II	9.3926(5)	3.33285(10)	13.1269(7)	77.329(5)	400.92(2)	3.51	1.020
1	0.1	I	9.3332(8)	4.6196(4)	11.4456(9)	82.101(7)	488.80(4)	5.47	1.008
0	0	I	9.3308(8)	4.6415(4)	11.4721(10)	82.069(6)	492.10(9)	3.99	1.318

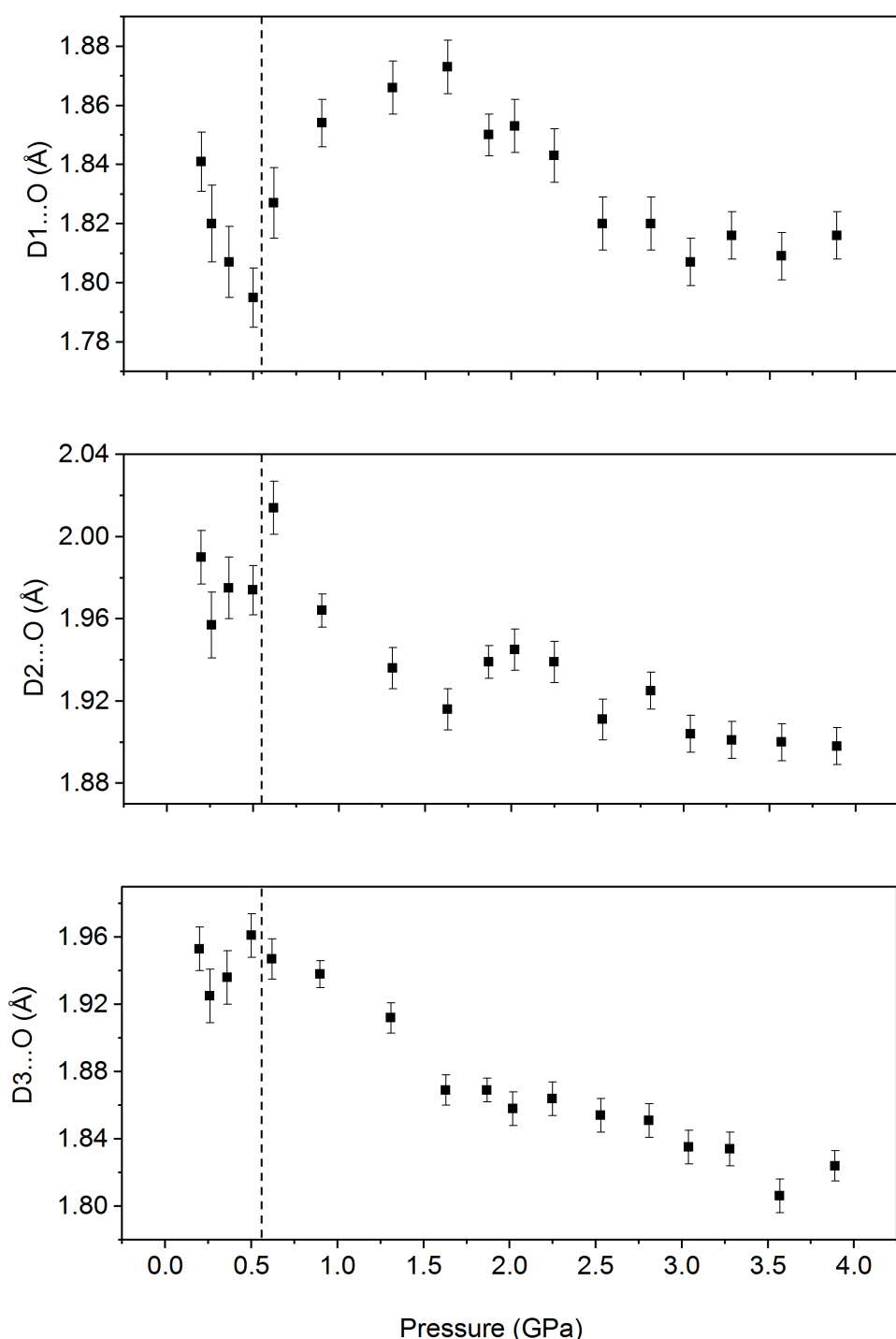


Figure S6: Variation in the three hydrogen bond D...O distances of perdeuterated biurea with increasing pressure. The dashed line indicates the pressure at which the phase transition from phase I to II occurs.

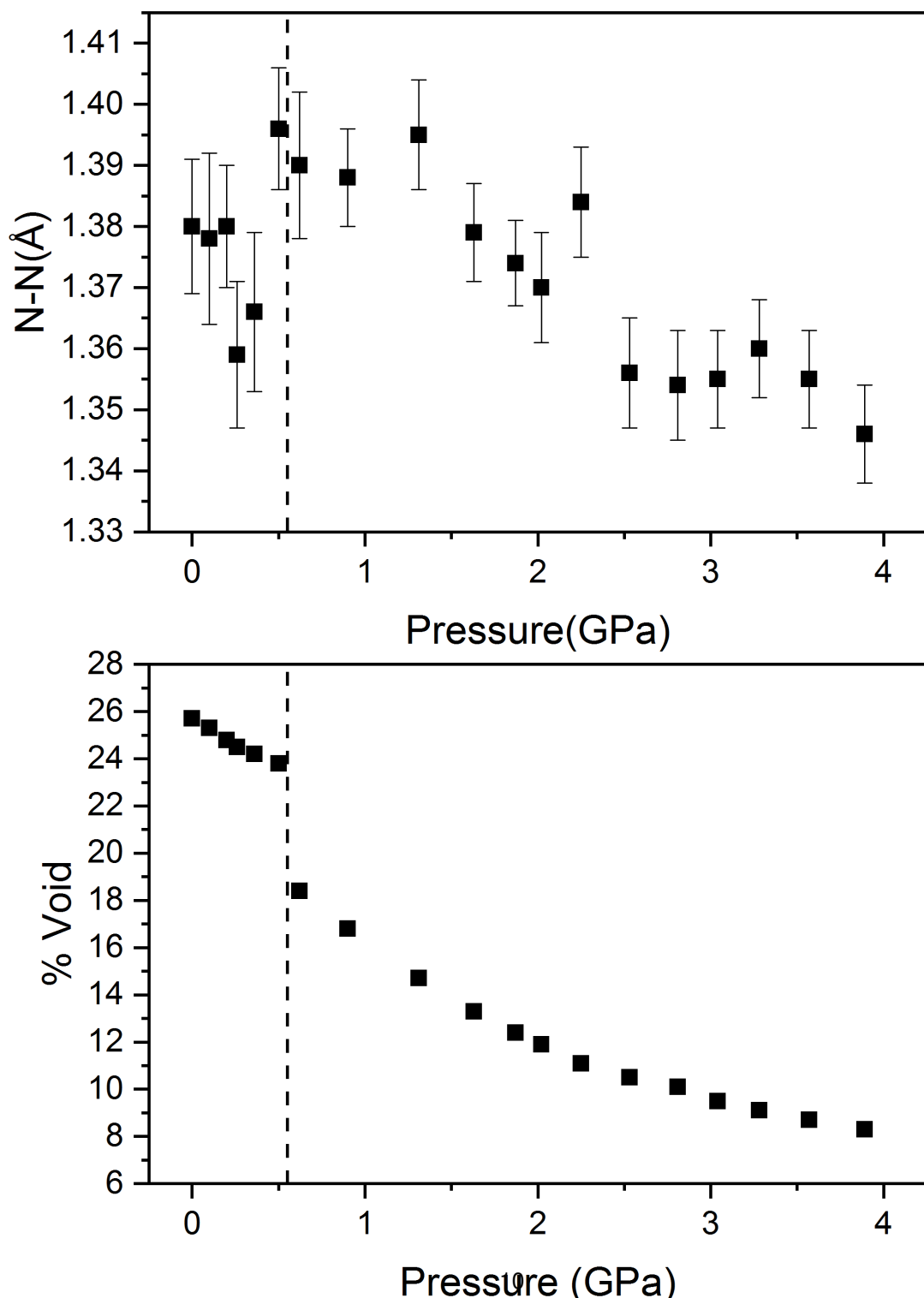


Figure S7: Top: Variation of the N–N distance in perdeuterated biurea with increasing pressure. Bottom: Variation in the % void of biurea with increasing pressure as determined by Mercury CSD 3.9 using 0.2 Å probe radii. The dashed line in both frames shows the pressure at which the phase transition from phase I to II occurs.

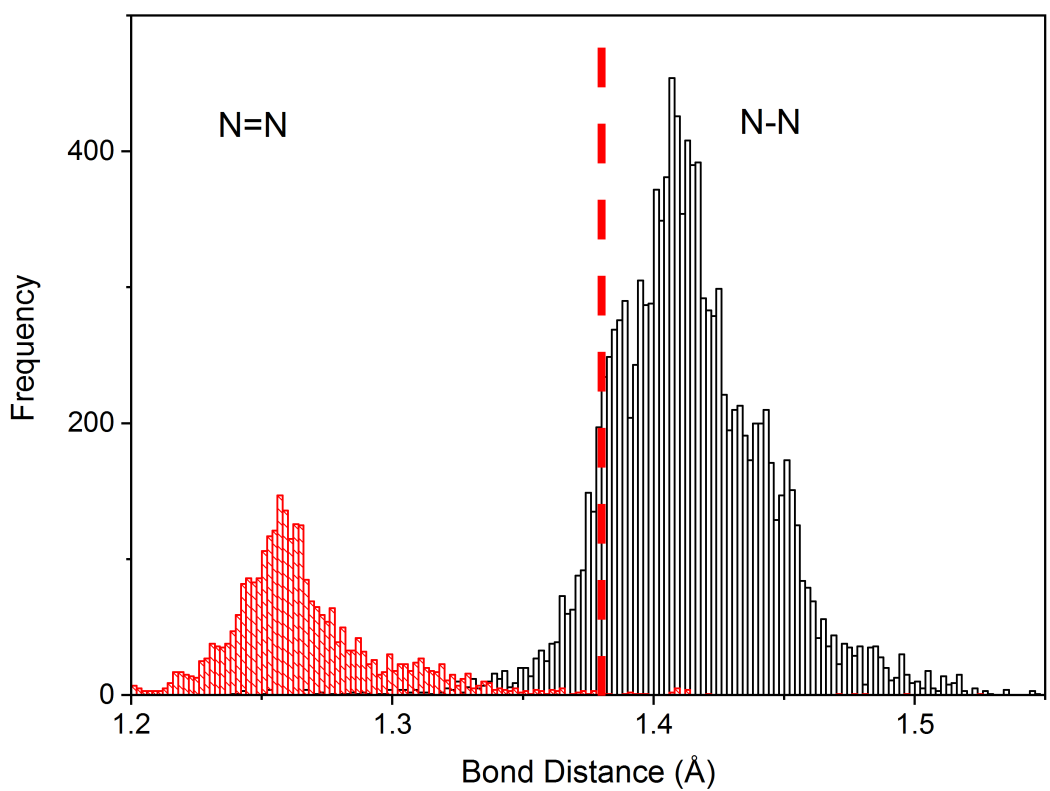


Figure S8: Values of N–N and N=N bond distance as reported in the CCDC database. The dashed line shows the value determined for biurea at ambient pressure.

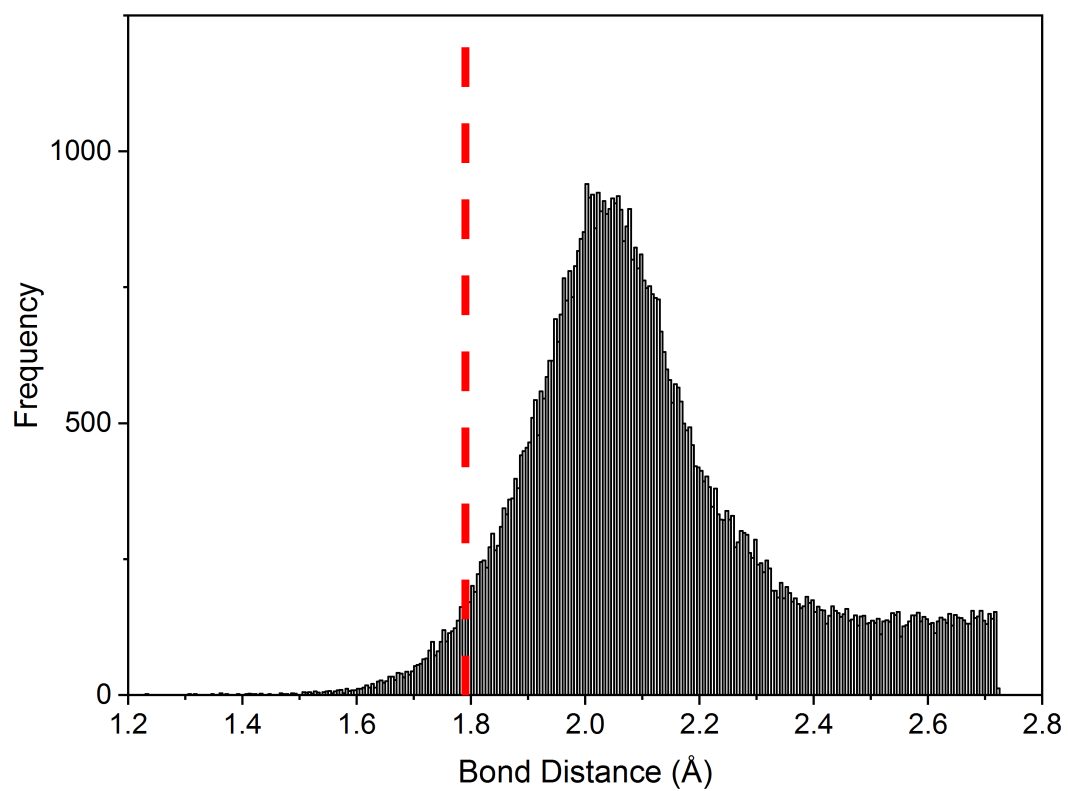


Figure S9: Values of H...O bond distance for N-H...O hydrogen bond lengths as reported in the CCDC. The dashed line shows the value of biurea at ambient pressure.

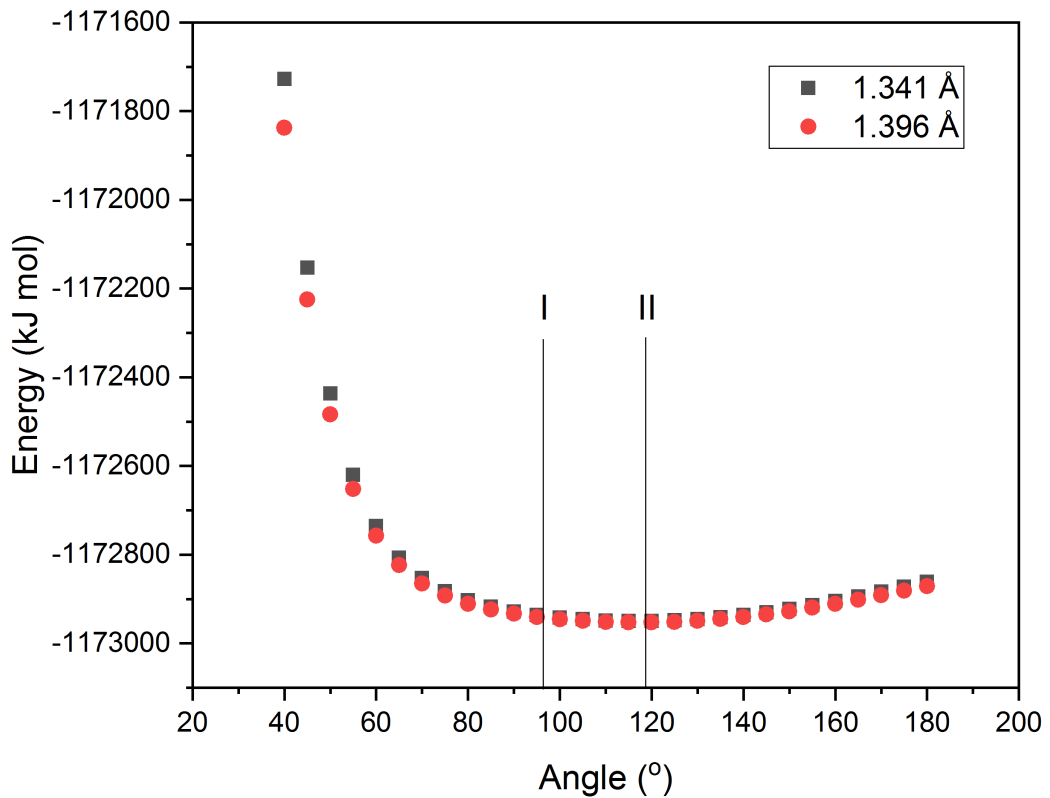


Figure S10: Variation in molecular configurational energy with torsion angle. *Ab-initio*, single point energy calculations in Gaussian, at the MP2 level, on a series of gas-phase molecules.^{S7} Each molecule was fixed to have identical geometry (informed by the ambient-pressure crystal structure), except for the flexible torsion angle, which was systematically varied in steps of 5° between 40 and 180°. The calculations were performed with N–N distances of 1.341 and 1.396 Å.

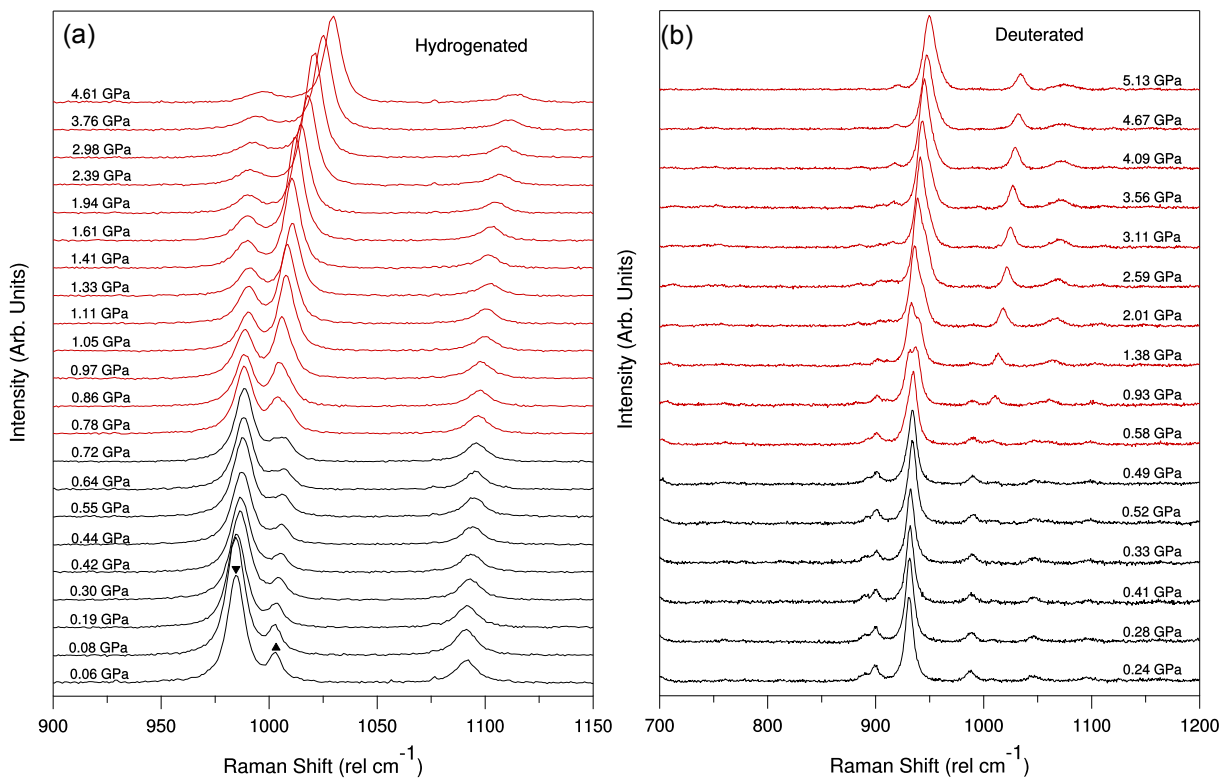


Figure S11: Raman spectra of biurea with increasing pressure. Left: Raman of perhydrogenated biurea around the region of the C–N stretch (○) and C–N–N (+) bending modes. Left: Same region of the Raman spectra for of perdeuterated biurea, the modes are shifted to lower wavenumber as a result of mass effects. In the two panels spectra in black are from the phase I and red from phase II.

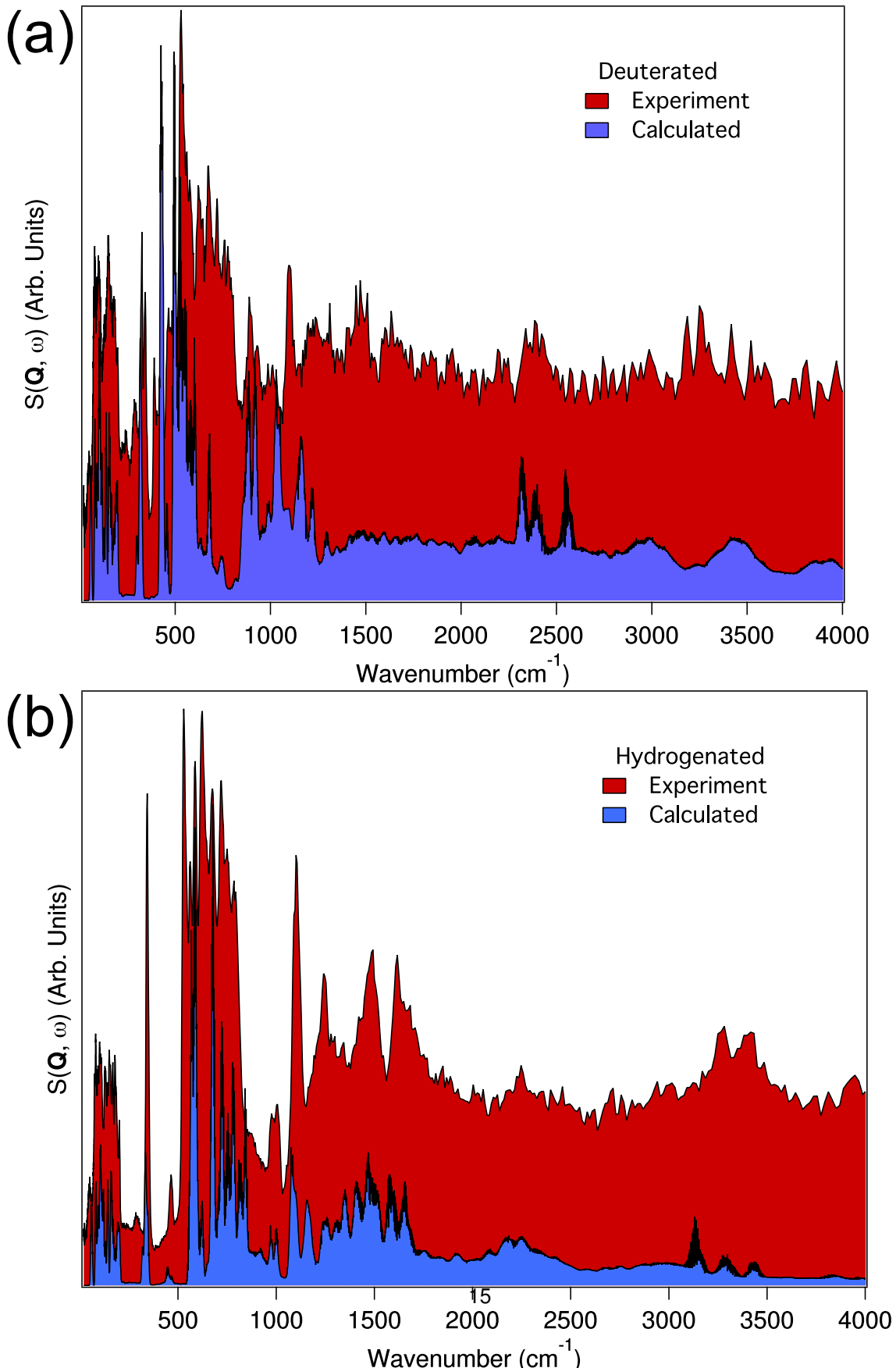


Figure S12: Experimental (red) and theoretical (blue) INS spectra of perdeuterated(a) and perhydrogenated(b) biurea. The spectrum from the perdeuterated sample is intrinsically noisier compared to the perhydrogenated sample as a result of the significant difference in scattering cross section of deuterium (7.64 barn) compared to that of hydrogen (82.03 barn).

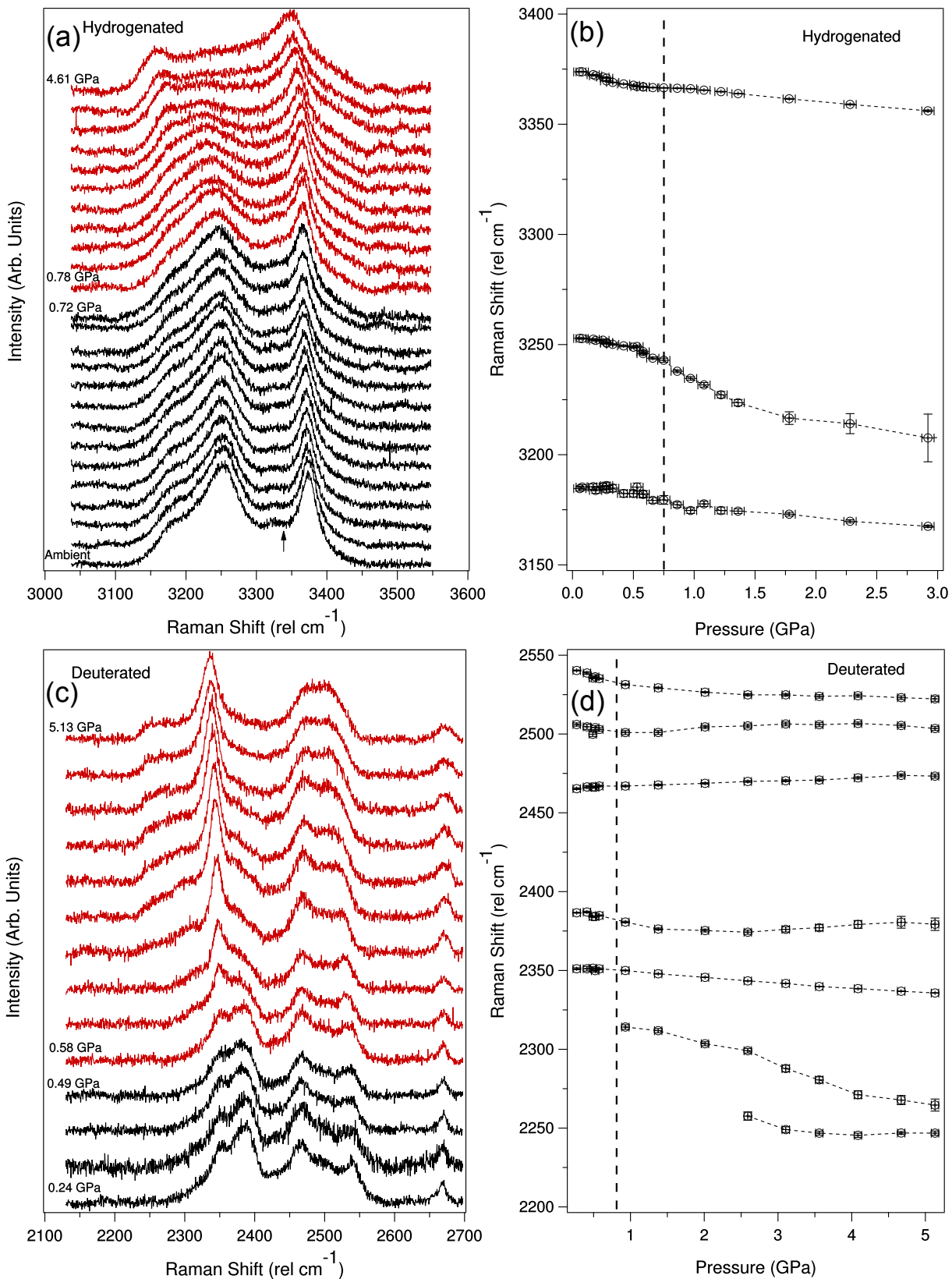


Figure S13: Raman spectra of biurea with increasing pressure. a: Variation in spectra around N–H stretching vibrational modes region for perhydrogenated sample . b: Determined peak positions as a function of pressure determined from a. c: Variation in spectra around N–D stretching vibrational modes region for perdeuterated sample. d: Determined peak positions as a function of pressure determined from c.

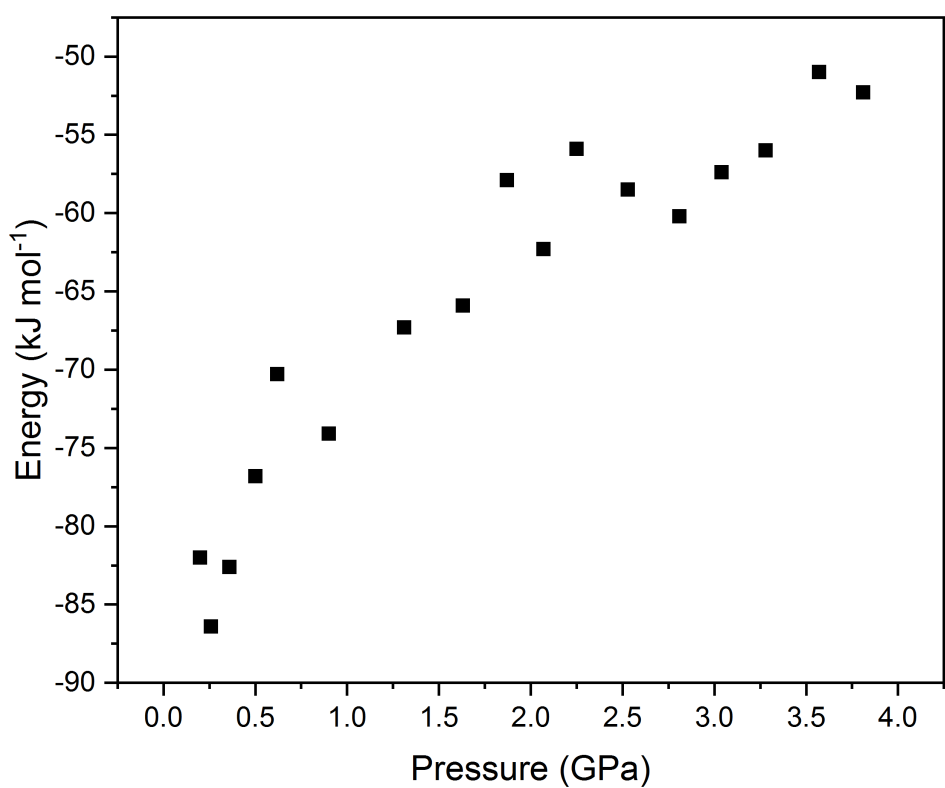


Figure S14: Lattice energy of experimental determined structures of Biurea with increasing pressure. Calculated using Gavezzotti's PIXEL method (A. Gavezzotti, *The Journal of Physical Chemistry B*, **107**, 10, 2344–2353 (2003)).